

Fig. 2 Time-dependent variation of vortex breakdown location for a) low-amplitude suction coefficient  $C_\mu = 0.09$ , suction probe at  $x_p/C = 1.06$ ; and b) large-amplitude suction coefficient  $C_\mu = 0.76$ , suction probe located at  $x_p/C = 1.0$ ,  $Re = 3.1 \times 10^4$ .

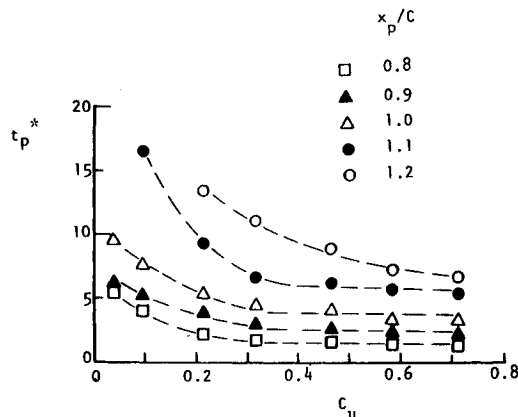


Fig. 3 Response time  $t_p^*$  for stabilization of vortex after onset of suction as a function of momentum coefficient  $C_\mu$  at various chordwise locations  $x_p/C$  of the suction probe.

point sink, since the probe tends to draw fluid from essentially all directions when located within the low-velocity recirculation zone of the vortex breakdown region. When the probe is located upstream of the trailing end of the wing ( $x_p/C < 1$ ), the impermeable surface of the wing causes a different sink flow pattern than that resulting from the probe located downstream ( $x_p > 1$ ) of the wing. The former pattern is apparently more efficient than the latter in removing the low-velocity fluid in the breakdown region, associated with movement of the vortex breakdown in the downstream direction.

Regarding the minimum value of suction coefficient  $C_\mu$  that produces stabilization of the core, it is obviously a strong function of the probe location relative to the position of vortex breakdown in the absence of suction. For breakdown at  $x_p/C = 0.45$  in the absence of suction and a probe location at  $x_p/C = 1.0$ , values of suction coefficient as low as  $C_\mu = 0.035$

allowed restabilization of the flow. Considerably lower values of  $C_\mu$  are expected to be effective when the tip of the probe is located further upstream, closer to the onset of vortex breakdown.

### Acknowledgment

This research effort is the by-product of a program sponsored by the Air Force Office of Scientific Research; the authors wish to express their appreciation for this support.

### References

- <sup>1</sup>Shi, Z., Wu, J. M., and Vakili, A. D., "An Investigation of Leading-Edge Vortices on Delta Wings with Jet Blowing," AIAA Paper 87-0330, Jan. 1987.
- <sup>2</sup>Visser, K. D., Iwanski, K. T., Nelson, R. C., and Ng, T. T., "Control of Leading-Edge Vortex Breakdown by Blowing," AIAA Paper 88-0504, Jan. 1988.
- <sup>3</sup>Bradley, R. G., Whitten, P. D., and Wray, W. O., "Leading Edge Vortex Augmentation in Compressible Flow," *Journal of Aircraft*, Vol. 13, April 1976, pp. 238-242.
- <sup>4</sup>Seginer, A. and Salomon, M., "Augmentation of Fighter Aircraft Performance by Spanwise Blowing over the Wing Leading Edge," NASA TM 84330, March 1983; AGARD-CP-341 Paper 33, 1983.
- <sup>5</sup>Werle, H., "Sur l'éclatement des tourbillons d'apex d'une aile delta aux faibles vitesses," *La Recherche Aéronautique*, No. 74, 1960.
- <sup>6</sup>Atta, R. and Rockwell, D., "Leading-Edge Vortices on a Pitching Delta Wing," *AIAA Journal*, Vol. 28, 1990.

## Effect of Surface Grooves on Base Pressure for a Blunt Trailing-Edge Airfoil

Gregory V. Selby\* and Farid H. Miandoab†  
Old Dominion University, Norfolk, Virginia

### Nomenclature

- $A$  = model base area
- $C_{pb}$  = local base pressure coefficient,  $(p - p_{ref})/q_\infty$
- $\bar{C}_{pb}$  = average base pressure coefficient
- $D$  = groove depth
- $d$  = diameter
- $q_\infty$  = freestream dynamic pressure,  $0.5 \rho_\infty V_\infty^2$
- $Re_L$  = Reynolds number based on chord length
- $s$  = model span
- $V_\infty$  = freestream flow speed
- $z$  = spanwise coordinate measured from the left end of model as viewed from downstream
- $\alpha$  = groove half angle
- $\Delta \bar{C}_{pb}$  =  $[\bar{C}_{pb} - (\bar{C}_{pb})_{baseline}] / (\bar{C}_{pb})_{baseline}$
- $\delta$  = boundary-layer thickness (based on ratio of local velocity to freestream velocity equal to 0.99)

Received Jan. 23, 1989; revision received Sept. 8, 1989. Copyright © 1990 American Institute of Aeronautics and Astronautics, Inc. No copyright is asserted in the United States under Title 17, U.S. Code. The U.S. Government has a royalty-free license to exercise all rights under the copyright claimed herein for Governmental purposes. All other rights are reserved by the copyright owner.

\*Associate Professor, Department of Mechanical Engineering and Mechanics. Senior Member AIAA.

†Graduate Research Assistant, Department of Mechanical Engineering and Mechanics.

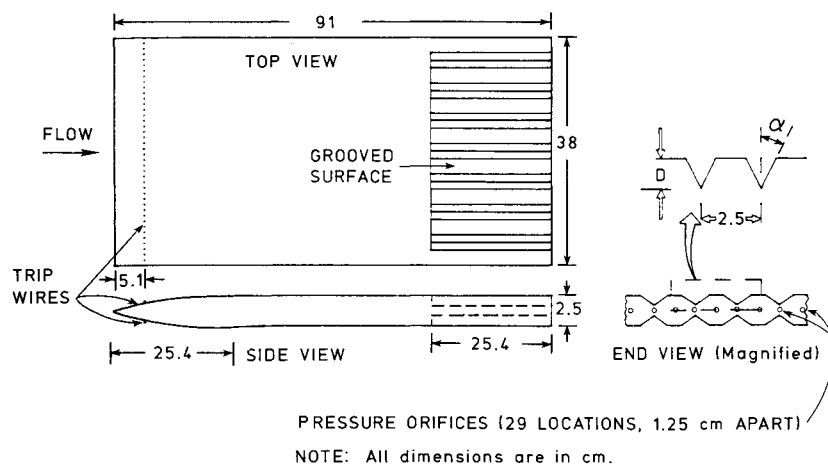


Fig. 1 Schematic of model.

### Introduction

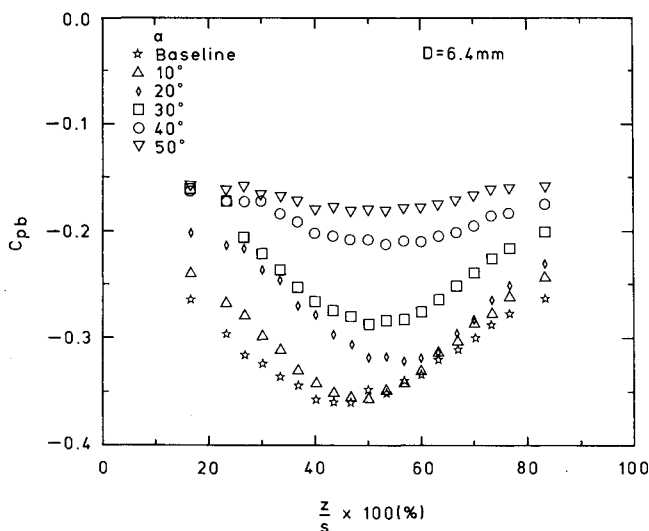
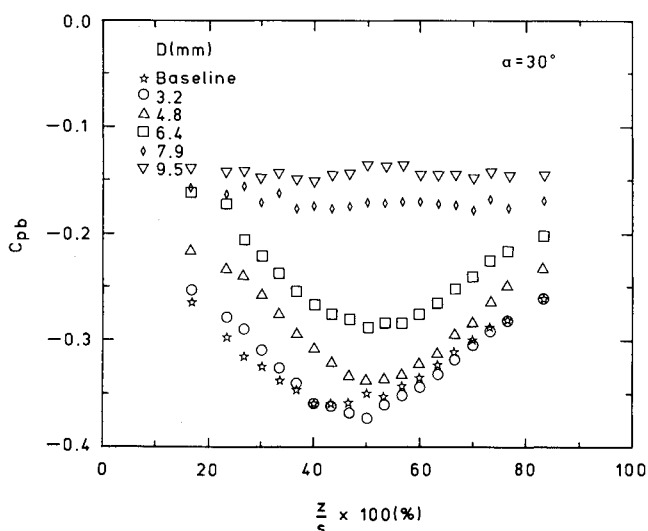
**F**LOW in the base region of a blunt trailing-edge airfoil at low speeds is dominated by a Karman vortex street. This region of low pressure contributes significantly to the total drag of the blunt body. Various techniques for increasing the base pressure of a blunt body by affecting the formation and strength of the periodically shed vortices have been investigated by aerodynamicists.<sup>1</sup> Some of these techniques include the addition of a splitter plate,<sup>2</sup> base geometry changes,<sup>3,4</sup> and base bleed.<sup>5</sup>

Previous research with V-shaped grooves has shown that they generate vortices parallel to the groove axis.<sup>6</sup> Minimally, attached flow has been shown to be present in the grooves.<sup>7</sup> Such an effect could be utilized to energize the flow in the base region of a blunt body by directing fluid of higher momentum into the weak base flow. This could also interfere with the formation of the Karman vortex street. The present study was conducted to examine the effect of longitudinal grooves on the base pressure of a flat-plate airfoil with a thick trailing edge.

### Experimental Setup and Measurements

Tests were conducted in the 0.91 m × 1.22 m test section of the Old Dominion University closed-loop, low-speed wind tunnel. An aluminum flat-plate airfoil with an elliptical leading edge, maximum thickness of 2.5 cm, span of 0.38 m, and

chord length of 0.91 m was the test model (see Fig. 1). A total of 73 pressure taps ( $d = 0.37$  mm) were incorporated in the design of the model to measure the pressure on the upper, lower, and base surfaces of the model. The model was supported in the test section by two 0.81-m high by 0.91-m long plexiglass end plates that were designed to isolate the test-section sidewall boundary layers and to help provide two-dimensional test conditions. Flow over the model was also separated from the test-section ceiling and floor boundary layers by attaching two horizontal 0.38-m wide by 0.91-m long plexiglass plates to the model vertical end plates at a distance of 0.30 m from the model surfaces. Freestream flow speeds were measured by two pitot-static probes mounted on the model end plates 12.7 cm above and below the model surfaces, just downstream of the elliptical leading edge. All base pressure measurements were referenced to the upper surface freestream static pressure. Provisions were made in the design of the model to allow insertion of the grooved surface over the downstream 25.4 cm of the model. To provide turbulent flow over the model, flow on both the upper and lower surfaces of the model was tripped by attaching wires ( $d = 1.02$  mm) 5.1 cm downstream of the leading edge.<sup>8</sup> Tests were conducted at zero model angle of attack and speeds of 17 and 42 m/s ( $Re_L = 10^6$  and  $2.5 \times 10^6$ , respectively). Velocity surveys of the boundary layers on the upper and lower surfaces of the model

Fig. 2 Local base pressure coefficient vs nondimensional spanwise position for various groove angles ( $V_\infty = 42$  m/s,  $D = 6.4$  mm).Fig. 3 Local base pressure coefficient vs nondimensional spanwise position for various groove depths ( $V_\infty = 42$  m/s,  $\alpha = 30$  deg).

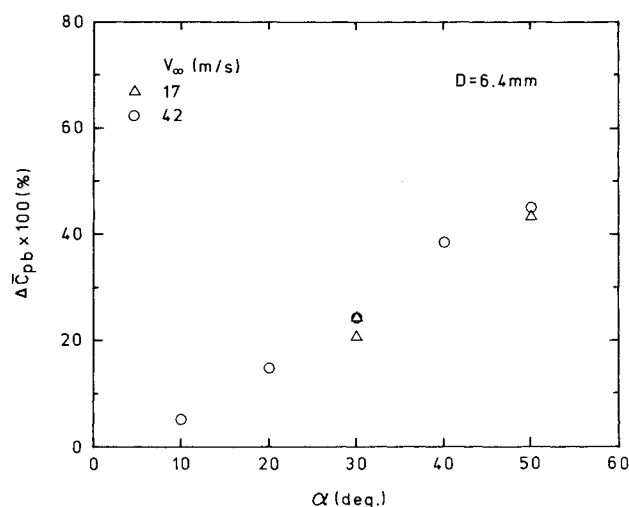


Fig. 4 Variation in average base pressure coefficient vs groove angle ( $D = 6.4$  mm).

at 2.5 cm upstream of the base indicated fully developed turbulent boundary layers for  $V_{\infty} = 17$  m/s ( $\delta$  for upper and lower surfaces of 1.7 and 1.8 cm, respectively). Transverse velocity surveys at the same location indicated the presence of two-dimensional flow over the model between  $z/s = 0.25$  and 0.75. Variations in freestream static pressure between the upper and lower surfaces correspond to variations in  $V_{\infty}$  of 1.3% at 17 m/s and 3% at 42 m/s. Model base pressure was measured using 25 pressure taps located along the centerline of the model base. In order to determine the effects of groove angle and groove depth on base pressure, models were tested with groove angles of 10 to 50 deg and groove depths of 3.2 to 9.5 mm ( $D/\delta$  of 0.2 to 0.6).

### Results and Discussion

Base pressure coefficient  $C_{pb}$  is presented in Figs. 2 and 3 ( $V_{\infty} = 42$  m/s) as a function of the nondimensional distance in the spanwise direction for variable groove angle tests and variable groove depth tests, respectively. It is evident from these figures that as groove angle or groove depth increases, the base pressure also increases. The data exhibit three-dimensional (end) effects that diminish as  $\alpha$  (or  $D$ ) increases. Asymmetries about the model centerline ( $z/s = 0.5$ ) are also noted. Tests with extended sidewalls have shown these to be largely due to three-dimensional end effects. Maximum increases in base pressure (50 to 60%) were obtained with  $\alpha = 50$  deg ( $D = 6.4$  mm) and  $D = 9.5$  mm ( $\alpha = 30$  deg) (see Figs. 2 and 3).

The average base-pressure coefficient  $\bar{C}_{pb}$  for each geometry tested was calculated from the  $C_{pb}$  data using area weighting. Percent changes in  $\bar{C}_{pb}$  from the baseline model for the groove angle tests are presented in Fig. 4 for freestream flow speeds of 17 and 42 m/s. The data indicate an almost linear increase in  $\bar{C}_{pb}$  with increasing  $\alpha$ . (A similar trend with increasing  $D$  was obtained). Overlapping of data from the two different Reynolds number tests suggests the independence of the base pressure increases from  $Re$  over the test range. In general, the data presented suggest the presence of a relationship between the groove dimensions and the strength of the interaction between the flow in the grooves and the wake flow.

### Conclusions

The results reported herein clearly indicate that the base pressure of a blunt trailing-edge airfoil with surface grooves increases with increasing groove depth and angle. Minimally, attached flow in the grooves appears to be the mechanism by which fluid of higher momentum is redirected to the base flow region to effect an increase in the base pressure. A study of the effect of grooves on the lift and total drag of blunt trailing-

edge airfoils is needed to further determine their effectiveness in this important application.

### Acknowledgment

The subject research was supported by the National Science Foundation under grant MSM 8519116.

### References

- <sup>1</sup>Hefner, J. N., and Bushnell, D. M., "An Overview of Concepts for Aircraft Drag Reduction," *Special Course on Concepts for Drag Reduction*, NATO Advisory Group for Aerospace Research and Development, AGARD Rpt. No. 654, 1977.
- <sup>2</sup>Nash, J. F., Quincy, V. G., and Callinan, J., "Experiments on Two Dimensional Base Flow at Subsonic and Transonic Speeds," London: Her Majesty's Stationery Office, National Physical Laboratory, Aerodynamics Division, NPL Aero. Rpt. 1070-A.R.C. 25 070, 1963.
- <sup>3</sup>Werle, M. J., Paterson, R. W., and Presz, W. M., Jr., "Trailing-edge Separation/Stall Alleviation," *AIAA Journal*, Vol. 25, No. 4, 1986, p. 624.
- <sup>4</sup>Gai, S. L., and Sharma, S. D., "Vortex Shedding from a Segmented Blunt Trailing-edge Aerofoil in Subsonic Flow," *Proceedings: 9th Australasian Fluid Mechanics Conference*, Auckland, New Zealand: University of Auckland, Dec. 1986, pp. 371-374.
- <sup>5</sup>Wood, C. J., "The Effect of Base Bleed on a Periodic Wake," *Journal of the Royal Aeronautical Society*, Vol. 68, July 1964, pp. 477-482.
- <sup>6</sup>Zumwalt, G. W., "Experiments on Three-Dimensional Separating-and-Reattaching Flows," AIAA Paper 81-0259, Jan. 1981.
- <sup>7</sup>Lin, J. C., Howard, F. G., and Selby, G. V., "Turbulent Flow Separation Control Through Passive Techniques," AIAA Paper 89-0976, March 1989.
- <sup>8</sup>Schlichting, H., *Boundary-Layer Theory*, McGraw-Hill, New York, 7th ed., 1987, p. 539.

## Unsteady Transonic Cascade Flow with In-Passage Shock Wave

C.-C. Li\*

Chung Shan Institute of Science and Technology,  
Taoyuan, Taiwan, Republic of China

and

A. F. Messiter† and B. van Leer‡

University of Michigan, Ann Arbor, Michigan

### Introduction

IN Ref. 1, asymptotic solutions were obtained for unsteady transonic flow in a channel with oscillating walls, for small reduced frequency. It was noted that an oscillating shock wave within the channel causes a time-dependent pressure force having a component in phase with the velocity of the walls,

Received Feb. 7, 1989; revision received July 10, 1989. Copyright © 1989 by the American Institute of Aeronautics and Astronautics. All rights reserved.

\*Assistant Research Scientist. Member AIAA.

†Professor, Department of Aerospace Engineering. Associate Fellow AIAA.

‡Professor, Department of Aerospace Engineering. Member AIAA.